Efficient Parallel Spatial Skyline Evaluation Using MapReduce

Wenlu Wang[†], Ji Zhang[†], Min-Te Sun[‡], Wei-Shinn Ku[†]

[†] *Department of Computer Science and Software Engineering, Auburn University, Auburn, AL, USA*
[‡] *Department of Computer Science and Information Engineering, National Central University, Taoyuan, Taiwan, ROC*
{wenluwang, jizhang, weishinn}@auburn.edu, msun@csie.ncu.edu.tw

ABSTRACT

This research presents an advanced MapReduce-based parallel solution to efficiently address spatial skyline queries on large datasets. In particular, given a set of data points and a set of query points, we first generate the convex hull of the query points in the first MapReduce phase. Then, we propose a novel concept called independent regions, for parallelizing the process of spatial skyline evaluation. Spatial skyline candidates in an independent region do not depend on any data point in other independent regions. Thus, we calculate the independent regions based on the input data points and the convex hull of the query points in the second phase. With the independent regions, spatial skylines are evaluated in parallel in the third phase, in which data points are partitioned by their associated independent regions in the map functions, and spatial skyline candidates are calculated by reduce functions. The results of the spatial skyline queries are the union of outputs from the reduce functions. Due to high cost of the spatial dominance test, which requires comparing the distance from data points to all convex points, we propose a concept of pruning regions in independent regions. All data points in pruning regions can be discarded without the dominance test. Our experimental results show the efficiency and effectiveness of the proposed parallel spatial skyline solution utilizing MapReduce on large-scale real-world and synthetic datasets.

Categories and Subject Descriptors

H.2.8 [**Database Management**]: Database Application—*spatial databases*

Keywords

Spatial Skyline Query, MapReduce, Parallel Computation

1. INTRODUCTION

Since the skyline operator was introduced into database research [4], a number of efficient algorithms have been proposed for the skyline evaluation. Bitmap [25], Index [25], NN (Nearest Neighbor) [16] and BBS (Branch-and-Bound Skyline) [19] rely on indices constructed before query processing; while BNL (Block Nested Loop) [4], D&C (Divide and Conquer) [4], SFS (Sort Filter Skyline) [7], and OSPS (Object-based Space Partitioning Skyline) [32] use non-index techniques. Moreover, several studies primarily focus on the skyline query in a variety of problem settings (data residing in a data stream [22] or on mobile devices [14]).

As a novel type of skyline queries, Spatial Skyline Query (SSQ) was proposed to consider the preference of both static and dynamic object attributes in multi-criteria decision-making applications [23]. Unlike skyline queries that only take static object attributes (e.g., rating and price of restaurants) into account, the distance between objects is also calculated as dynamic attributes in the spatial skyline queries. In particular, given a set of data points P and a set of query points Q in a d-dimensional space, spatial skyline queries return a subset of P, in which data points are not spatially dominated by other data points in P. The spatial dominance is defined by using the distance from data points to all query points.

Spatial skyline query is applicable to many applications. Take crisis management applications as an example, we assume that a number of waterborne infectious disease cases were confirmed at different locations, people who live at spatial skyline places with respect to those locations should be alerted and examined first, because there might be higher possibility that these people may have been exposed to contagious water. Travel planning applications are another type of example. People may prefer the spatial skyline hotels with respect to fixed locations of beaches and museums for their vacation. In this case, people would not like to choose a hotel, which is farther from all interesting attractions than other hotels. One more example of spatial skyline query is that people may plan to have dinner with their friends at weekends. They may consider the distance from their homes to the restaurant for the restaurant selection. The restaurants far from all of their homes would not be in the candidate list, because they may want to save time on the road. Thus, giving a list of spatial skyline restaurants is the first step of the restaurant selection.

Two index-based algorithms were proposed to efficiently address the spatial skyline queries [23]. Branch and Bound Spatial Skyline B^2S^2 algorithm searches spatial skyline candidates by visiting an R-tree from top to bottom. Once a spatial skyline is found, B^2S^2 expands the R-tree to access the node which has minimum mindist value, and compares it with all spatial skyline candidates found so far in spatial dominance test. The other method, Voronoi-based Spatial Skyline VS^2 algorithm relies on a Voronoi diagram created over input data points. VS^2 starts with the closest data points to query points, searches in the space by visiting the neighbors of visited data points over the Voronoi diagram. Due to high cost of the spatial dominance test, VS^2 was improved by reducing the number of spatial dominance tests in [24]. In the method, seed skyline points (a subset of spatial skyline points) can be identified with spatial dominance test.

However, the following problems motivate us to propose a novel parallel solution for spatial skyline evaluation. Firstly, as data grows rapidly, addressing skyline queries on large-scale datasets in a single-node environment becomes impractical. There are increasing number of approaches proposed for processing skyline queries in distributed and/or parallel environments [13]. But none of parallel spatial skyline solutions were observed in literature. Secondly, the distance between moving objects may keep changing. If indices are created at a preprocessing stage, the cost of index maintenance would be unacceptably high. Thirdly, MapReduce framework has been incorporated into parallel solutions for skyline computation [17] [20] [31] and other database applications [30] [26] [18].

Therefore, we propose a novel three-phase MapReduce-based solution, which is able to efficiently address spatial skyline queries on large-scale datasets in this paper. In particular, given a set of data points and a set of query points, we calculate the convex hull of the query points in the first phase. Initially, the query points are evenly partitioned. Each map function accepts a subset of query points, and outputs a local convex hull. Then, the reduce function produces the global convex hull by merging the intermediate results from the map functions. A filtering method can be applied to filter out unqualified data points before the convex hull computation. For example, CG_Hadoop uses skyline algorithms as a filtering method in convex hull evaluation [11]. Moreover, to parallelize the spatial skyline computation, we propose a novel concept, independent regions, in each of which spatial skylines do not depend on any data point outside the independent region. If data points do not fall in any independent region, they can be discarded because they must be spatially dominated by other data points. Thus, our solution produces the independent regions at the second phase. Each map function receives a subset of data points and the convex hull of query points, and generates locally optimized independent regions. Then, the reduce functions output globally optimized independent regions.

With the independent regions in the third phase, map functions associate data points with their independent regions. By using the unique identifiers of independent regions as keys, all data points in an independent region are sent to a reducer after the shuffle phase, and reduce functions find the spatial skylines in independent regions in parallel. Due to high cost of the spatial dominance test, which requires comparing the distance from data points to all convex points, we propose a novel concept, pruning regions, in independent regions. The pruning regions are the areas in which all data points are dominated by other data points. Thus, since a pruning region is defined by a data point, a convex point, and its adjacent convex points, if a data point is in a pruning region, the data point can be discarded without accessing all convex points and calculating the distance from the data point to them. In addition, a data point may fall in more than one independent regions, and there may exist duplicates in spatial skyline candidates. We employ an elimination method in our solution to remove the duplicates with subtle overhead.

In short, the contributions of this study are summarized below:

1. We propose a parallel scheme to efficiently evaluate spatial skyline queries on large datasets using MapReduce.

2. We introduce a concept of independent regions in our solution. The spatial skyline candidates in an independent region do not depend on any data points in other independent regions. With the feature of the independence, spatial skyline queries can be addressed in parallel.

3. We present a concept of pruning regions in independent regions, in order to minimize the cost of the dominance test by avoiding the computation of distance from data points to all convex points.

4. We evaluate the performance of the proposed solution through extensive experiments with large-scale real-world and synthetic datasets.

The rest of this paper is organized as follows. Section 2 surveys related works. The spatial skyline queries and relevant techniques utilized in our solutions are formally defined in Section 3. In Section 4, our advanced solution is presented. The experimental validation of our design is presented in Section 5. We conclude the paper in Section 6.

2. RELATED WORK

In this section, we review previous works related to spatial skyline queries and parallel solutions for general skyline queries.

2.1 Spatial Skyline Queries

As a special case of dynamic skyline queries, Spatial Skyline Queries (SSQ) can be addressed by Block Nested Loop (BNL) [4] and Branch-and-Bound Skyline algorithms (BBS) [19]. In a dynamic skyline query, each object is mapped to another search space by using pre-defined functions. All the objects that are not dominated by other objects in the search space after the mapping are returned from the dynamic skyline queries. BNL algorithm can address the dynamic skyline queries, because it compares every pair of objects in the input dataset, and eliminates the ones that are dominated by any other objects. BNL does not need indices and is efficient over small datasets. But it suffers from I/O access when the input datasets become large. If the size of skyline candidates exceeds the size of available memory space, all the candidates have to be written to a temporary data stream, and read back when they are needed in the next iteration of object comparison. BBS relies on an R-tree to evaluate the general skyline queries; it calculates the $mindist$ of intermediate entries in the R-tree, and searches the space by expanding the entry with the smallest $mindist$. However, BBS does not consider the relation between the input query points and data points.

Motivated by the inefficiency of BNL and BBS, a Branch-and-Bound Spatial Skyline (B^2S^2) algorithm and a Voronoi-based Spatial Skyline (VS^2) algorithm were proposed for spatial skyline evaluation [23]. In addition to considering the properties of the convex hull generated by input query points, B^2S^2 searches the space by visiting an R-tree from top to bottom. Once the first spatial skyline is found, B^2S^2 expands the R-tree with the node which has the minimum $mindist$ value, and checks the dominance between the visited node and all spatial skyline candidates found so far. The process continues until all intermediate nodes potentially containing spatial skylines have been visited. On the other hand, VS^2 builds a Voronoi diagram over input data points. The input data points are organized by their Hilbert values in pages in order to preserve their locality. After completion of convex hull calculation, VS^2 starts with the closest data points to the query points, and searches the space by visiting the neighbors of visited data points over the Voronoi diagram. For every visited data point, VS^2 compares it with all spatial skylines found so far for spatial dominance test. The process continues until all Voronoi cells (or data points) that potentially contain spatial skylines have been visited. Inspired by high cost of the spatial dominance test, VS^2 was improved by reducing the number of spatial dominance tests [24]. In addition to applying sorting techniques, the method is able to identify seed skyline points (a subset of spatial skyline points) without dominance test. Given a set of query points Q and a set of data points P, let $V(p_i)$ be the Voronoi cell of data point $p_i \in P$, the seed skyline points are the points p_i that $V(p_i)$ intersect with the boundary of the convex hull of Q or is inside the convex hull. However, none of the aforementioned methods can address the spatial skyline query in parallel. B^2S^2 requires a pre-structured R-tree and VS^2 needs to build a Voronoi diagram over input data points. Extending their methods to a distributed and/or parallel environment is non-trivial.

2.2 Parallel Skyline Solution

Due to high cost of skyline evaluation, a number of advanced solutions have been proposed to evaluate the general skyline queries in a distributed and/or parallel environment. Balke *et al.* developed a parallel skyline solution over distributed environments [3]. Their method first vertically partitions input datasets in such a manner that each partition keeps object attributes in one dimension. Then, the skyline objects are calculated in parallel, and reported to a central point for a final dominance check. Wu *et al.* designed a parallel skyline method that leverages content-based data partitioning [28]. Their method can avoid unnecessary data access and can progressively produce skylines by using recursive region partitioning and dynamic region encoding mechanisms. Moreover, the incremental scalability is also provided in such a manner that workload can be automatically balanced by distributing objects to new nodes. In addition to random data partitioning methods that can generate similar data distribution in each partition [8] and grid-based data partitioning methods that consider object proximity [2] [21], Vlachou *et al.* proposed an angle-based data partitioning method that partitions objects by their angular coordinates [27]. The average pruning power of objects within a partition can be increased and the number of skyline objects in local skyline calculation can be minimized by applying the angle-based partitioning method. Köhler *et al.* designed a hyperplane-based data partitioning method in order to minimize the local skylines in a partition and achieve efficient local skyline merging [15]. Moreover, a variety of MapReduce-based parallel solutions have been proposed for skyline queries and other database applications. Han *et al.* proposed an advanced skyline algorithm that utilizes Sorted Positional Index Lists (SSPL) to reduce I/O cost [12]. Zhang *et al.* implemented BNL, SFS, and Bitmap algorithms using MapReduce framework [29]. Chen *et al.* applied an angular data partition in their MapReduce-based solution for skyline query evaluation [6]. Eldawy *et al.* developed CG_Hadoop, a suite of MapReduce algorithms, to solve fundamental computational geometry problems, which include convex hull computation [11]. Mullesgaard *et al.* investigated the general skyline queries by using the MapReduce framework. Their method uses bit strings to represent the dominance relation of attributes, and generates independent partition groups for calculating local skyline objects in parallel [17]. Zhang et al. proposed an efficient parallel skyline solution using MapReduce, in which a Partial-presort Grid-based Partition Skyline (PGPS) algorithm was developed to significantly improve the merging skyline computation on large datasets [31]. More importantly, PGPS can be easily incorporated in the shuffle phase of the MapReduce framework with minor overhead. However, our proposed solution targets on spatial skyline queries, which are different from the general skyline queries. None of the partition schemes or computation algorithms above could address the spatial skyline problem. Therefore, we propose a novel partition method and a parallel algorithm which includes independent regions to parallelize the spatial skyline computation and pruning regions to reduce the cost of spatial dominance test.

Table 1 Symbolic notations.

Symbol	Meaning
P, Q	a set of data points and a set of query points
p, q	a data point and a query point
$p.x_i$	the value of data point p in the i^{th} dimension
$\mathbb{R}^d$	a d-dimensional space
h	a hyper-place
S	a half-space
F	a facet of a convex hull
$A_q^{\triangle}$	a set of adjacent convex points of q
$p \prec^Q p'$	p spatially dominates p' with respect to Q
$SSKY(P, Q)$	spatial skylines of P with respect to Q
$CH(Q)$	the convex hull of Q
$DR(p, Q)$	the dominator region of p with respect to Q
$PR(p, q)$	the pruning region generated by p and q
$IR(p, q)$	the independent region generated by p and q
IRP	Independent Regions Pivot, the independent regions are generated by IRP
$lssky$	a set of local spatial skyline candidates
$chsky$	a set of spatial skyline candidates in a convex hull

3. PRELIMINARIES

3.1 Problem Statement

Given a dataset P in a d-dimensional space $\mathbb{R}^d$, an object $p \in P$ can be represented as $p = \{x_1, x_2, ..., x_d\}$ where $p.x_i$ is the value of the object on the i^{th} dimension. $D(.,.)$ denotes a distance metric that obeys the triangle inequality in $\mathbb{R}^d$. The spatial dominatnce relationship and the spatial skyline operator are defined as follows [23]. All notations used in this paper are summarized in Table 1.

Definition (*Spatial Domination*) Given a set of query points Q, and two data points p and p' in $\mathbb{R}^d$, p spatially dominates p' with respect to Q, denoted by $p \prec^Q p'$, if $\forall\, q \in Q,\ D(p, q) \le D(p', q)$ and $\exists\, q' \in Q,\ D(p, q') < D(p', q')$.

Definition (*Spatial Skyline*) Spatial skylines of a set of data points P with respect to a set of query points Q in $\mathbb{R}^d$, denoted by $SSKY(P, Q)$, are a set of data points in P, which are not spatially dominated by any other data point in P with respect to Q.

$$SSKY(P, Q) = \{p \in P \mid \nexists\, p' \in P, p \ne p', p' \prec^Q p\} \qquad (1)$$

PROPERTY 1. *If any data point $p \in P$ is a spatial skyline point with respect to a subset of query points $Q' \subset Q$, then p is also a spatial skyline point with respect to Q [23].*

PROPERTY 2. *The set of spatial skyline points of data points P does not depend on any non-convex query points $q \in Q$, $q \notin CH(Q)$, where $CH(Q)$ indicates the convex hull of Q [23]. In other words,*

$$SSKY(P, Q) = SSKY(P, CH(Q)) \qquad (2)$$

Definition (*Dominator Region*) Given a data point $p \in P$, a set of query points Q, and hyper-spheres that center at q_i with radius $D(p, q_i)$, $q_i \in Q$, any data point inside the intersection of the hyper-spheres spatially dominates p with respect to Q. The intersection area that potentially contains data points spatially dominating p with respect to Q is referred to as the dominator region of p, denoted by $DR(p, Q)$.

Dominator Region enables our solution to efficiently eliminate data points by reducing the search space of data points. For example, Figure 1 displays dominator region of a data point p and a set of query points Q. Q has three query points q_1, q_2, and q_3,

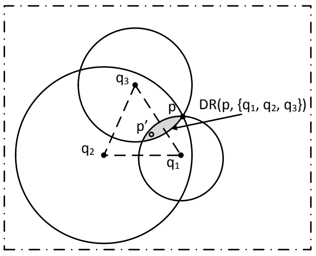

Figure 1: An example of $DR(p, \{q_1, q_2, q_3\})$ in a 2-dimensional space.

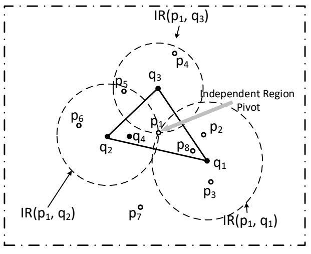

Figure 2: An example of Independent Regions in a 2-dimensional space.

which represent a convex hull in a 2-dimensional space. Three circles centered at $q_i \in Q$ with radius $D(q_i, p)$ are created in order to highlight the dominance areas of p with respect to the query points. Any data point p' in the intersection of the three circles spatially dominates p with respect to Q.

3.2 Convex Hull and Spatial Skyline Queries

Given a set of query points Q in a d-dimensional space $\mathbb{R}^d$, the convex hull of Q, denoted by $CH(Q)$, is the smallest convex polytope that contains all query points in Q. Theoretically, a convex hull can be represented as either a set of convex points or the intersection of a set of half-spaces. Each half-space contains all the query points in Q. Moreover, a convex hull can also be abstracted by a set of facets and their adjacency relationships. Each facet can be defined by a number of convex points. For example, a facet (line) can be determined by two adjacent convex points in a 2-dimensional space. The facets become planes that can be represented by a convex point and its two adjacent convex points in a 3-dimensional space. Because the facets of $CH(Q)$ separate the query points in Q from any point outside the convex hull, connecting a data point v outside $CH(Q)$ with any data point in $CH(Q)$ must intersect with at least one facet of the convex hull. Thus, the facet is referred to as a visible facet from v.

The properties of convex hull provide opportunities to optimize the process of spatial skyline evaluation by reducing the search space of both data points and query points. Given a set of data points P and the convex hull of a set of query points Q, all data points inside $CH(Q)$ are spatial skylines of P with respect to Q [23]. Given two data points, if they are in the convex hull, the bisector hyper-plane of these two points partitions the space into two half-spaces, and there must exist convex points in either half-space. Thus, neither of the two data points can spatially dominate the other, and both of them are spatial skylines. If one point p_1 is in the convex hull and the other p_2 is not, then, the bisector line of p_1 and p_2 partitions the space into two half-spaces, and there must exist a convex point in the same half-space with p_1. If the convex point does not exist, the convex hull cannot contain p_1, which contradicts with our assumption. Thus, p_1 is not spatially dominated by p_2. These two cases are summarized in Property 3.

PROPERTY 3. *Given a set of data points P and a set of query points Q, if any point $p \in P$ is inside the convex hull of Q, then p is a spatial skyline of P with respect to Q ($p \in SSKY(P, Q)$).*

3.3 MapReduce Overview

MapReduce was proposed as a generic programming model for data-intensive applications in distributed environments [10]. The framework provides two simple primitives, map and $reduce$ functions, and allows developers to mainly focus on their functionality. The task scheduling, load balancing, and other issues are encapsulated in the MapReduce framework, which significantly reduces the difficulty of the development of parallel applications. Driven by the MapReduce framework, map functions receive data in key/value pairs from input streams and output intermediate results in another type of key/value pairs. Then, $reduce$ functions retrieve the intermediate results and write final results to an output stream. In the shuffle phase, the intermediate results are automatically grouped and sorted by the MapReduce framework, The two primitives can be represented as: map(K_1, V_1) $\rightarrow$ list(K_2, V_2) and reduce(K_2, list(V_2)) $\rightarrow$ list(K_3, V_3).

4. DESIGN

In this section, we propose our advanced parallel spatial skyline solution using MapReduce. First of all, we briefly present the framework of the solution. Then, our spatial skyline algorithm is illustrated in detail in Section 4.2. The concepts of independent regions and pruning regions are introduced to optimize the process of spatial skyline evaluation. Finally, we discuss three critical implementation issues in our solution.

4.1 Framework Overview

Our solution consists of three MapReduce phases, which receive a set of data points P and a set of query points Q as inputs, and output spatial skyline points of P with respect to Q. As illustrated in Figure 3, we calculate the convex hull of Q in the first MapReduce phase. Q is initially partitioned into subsets of equal size, and each map function finds the local convex hull of query points in a subset. Then, a reduce function generates the global convex hull of Q by merging the local convex hulls. Convex hull algorithm like Graham scan could be employed in each map and reduce function [5]. Due to high complexity of convex hull computation, a filtering method can be used to filter out unqualified points with lower cost. For example, Eldawy *et al.* observed that the convex points must be at least one of four types of skyline points of Q (max-max, min-max, max-min, and min-min) in a 2-dimensional space, and applied skyline algorithms as a filtering step in their CG_Hadoop system [11].

An intuitive spatial skyline method requires to examine the spatial dominance between every pair of data points. Sharifzadeh and Shahabi utilized the R-tree and Voronoi diagram as indices in their B^2S^2 and VS^2 algorithms [23]. Son *et al.* enhanced VS^2 by reducing the number of dominance tests [24]. However, extending these methods to a parallel solution is non-trivial. Efficiently maintaining indices over data in a distributed and/or parallel environment requires expertise and extensive experience. To address this issue, we propose a novel concept, independent regions, in each of which spatial skyline points do not depend on any data points outside the independent region. With the independence, the input data points can be partitioned by their independent regions, and spatial skyline points can be calculated in parallel. Therefore, after the completion of convex hull computation, we calculate the independent regions based on the convex hull and the input data points P in the second phase. Each map function takes a subset of P and the convex hull of Q as inputs, and outputs a locally optimal **Independent Region Pivot** (See Figure 2, the independent regions are determined by the independent region pivot and convex points). Then a reduce function produces a globally optimal independent region pivot by merging the intermediate results. More details of independent region pivot selection will be discussed in Section 4.3.1. In the third phase, P is initially partitioned, and each map function finds the independent regions of data points in a split. The output of the map functions can be represented as $< IR.id, p >$, where $IR.id$ denotes the unique identifier of the independent region associated with a data point p. There are three possible cases: (1) data points

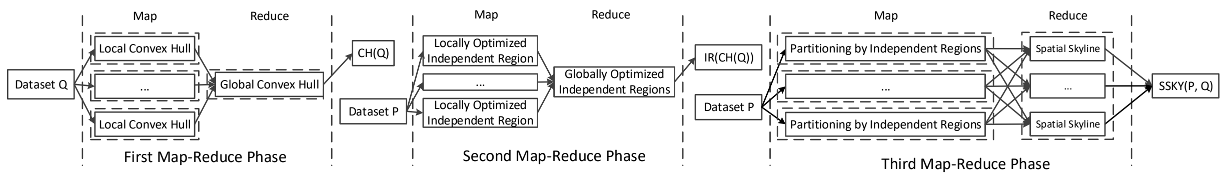

Figure 3: An overview of the parallel spatial skyline processing using MapReduce.

are eliminated if they are outside all independent regions; (2) data points are marked and output as spatial skylines by mappers and reducers if they are inside the convex hull of Q. These data points are needed in reduce functions, because they may spatially dominate data points in category 3; (3) data points are produced with their associated independent regions if they fall in at least one independent region. These data points will be processed by reducers to find spatial skylines in the independent regions. If a data point is inside two or more independent regions, the map function will produce a pair of $< IR.id,\ p >$ for every associated independent region. After the shuffle phase, data points in P are grouped by independent regions, and sent to reduce functions for spatial skyline calculation in parallel. Finally, the global spatial skyline points are the union of the output of reduce functions. A data point could be associated with two or more independent regions, which may introduce duplicates in the results. We design an elimination method to remove duplicates in our solution. The method will be presented in Section 4.3.3.

Figure 2 shows an example of spatial skyline query over three query points and eight data points (Q={q_1, q_2, q_3, q_4}, P={p_1, ..., p_8}). First of all, the convex hull of query points ($CH(Q)$) is generated in the first MapReduce phase. Then, the globally optimal independent region pivot is found by using P and $CH(Q)$ in the second MapReduce phase. Each mapper takes a split of P and $CH(Q)$ (a constant global variable), and selects a local optimal independent region pivot, and a reducer outputs the globally optimal pivot. In the third MapReduce phase, each mapper receives a split of P, and the pivot and $CH(Q)$ (as two constant global variables), and produces object points with their associated independent regions. In the example, there are three independent regions ($\{IR(p_1, q_1)$, $IR(p_1, q_2)$, $IR(p_1, q_3)\}$). All the independent regions can be calculated from the pivot and $CH(Q)$ in mappers. Moreover, object points are associated with the independent regions where they locate in. If we use ir_1, ir_2, and ir_3 to denote $IR(p_1, q_1)$, $IR(p_1, q_2)$, and $IR(p_1, q_3)$, then p_1 is associated with ir_1, p_5 is associated with ir_2 and etc. After the shuffle phase, $< ir_1, p_1 >$, $< ir_1, p_2 >$, $< ir_1, p_3 >$, and $< ir_1, p_8 >$ are grouped and sent to the first reducer, $< ir_2, p_1 >$, $< ir_2, p_5 >$, and $< ir_2, p_6 >$ are passed to the second reducer, and $< ir_3, p_1 >$ $< ir_3, p_4 >$ $< ir_3, p_5 >$ are processed in the third reducer. In this case, p_1 is a special object point, which is in all three independent regions. As we will discuss our elimination method in Section 4.3.3, p_1 will be only output by the first reducer. Thus, the first reducer outputs p_1, p_2 and p_8 as spatial skylines and discards p_3 because it is dominated by p_8. The second reducer produces p_5, p_6. The third reducer does not output any object because p_4 is eliminated in the spatial dominance test and p_5 has been produced in the second reducer. Finally, the result of the spatial skyline query is the union of the results of reducers, which are $\{p_1$, p_2, p_5, p_6, $p_8\}$.

4.2 Spatial Skyline Calculation

In the second and third MapReduce phases, we generate independent regions based on the convex hull of Q and a set of data points P for spatial skyline computation in parallel. In this subsection, we first provide a formal definition of an independent region. Due to high cost of the spatial dominance test that requires comparing the distance from data points to all convex points, we introduce pruning regions in independent regions. A pruning region can be defined by a data point inside $CH(Q)$, a convex point, and its adjacent convex points. If a data point is in a pruning region, the point can be discarded without the dominance test.

Definition (*Independent Region*) Given a data point p and a set of query points Q in a d-dimensional space, we define an *Independent Region* of p and q_i, $q_i \in Q$ as a sphere centered at q_i with radius $D(p, q_i)$. An **Independent Region Group** (IRG) of p with respect to Q is the union of the independent regions, as shown in Figure 2.

$$\begin{aligned} IRG(p, Q) &= \bigcup_{q_i \in Q} IR(p, q_i), \text{ where} \\ IR(p, q_i) &= \{l \mid D(l, q_i) \leq D(p, q_i)\} \end{aligned} \tag{3}$$

We define data point p as the **Independent Region Pivot** of $IRG(p, Q)$ as shown in Figure 2.

With the definition of the independent region, we provide the independence of spatial skylines as follows.

THEOREM 4.1. *Given a data point p and its independent regions* $\{IR(p, q_j) \mid q_j \in CH(Q)\}$*, where* $CH(Q)$ *is the convex hull of query points Q,* $\forall\ q_j \in CH(Q)$*, any data point* $p' \in IR(p, q_j)$ *is not dominated by any data point* $p'' \notin IR(p, q_j)$*.*

PROOF. The proof is by contradiction. Assume that $\exists\ p' \in IR(p, q_j)$, $p'' \notin IR(p, q_j)$, $p'' \prec^Q p'$. By the definition of spatial skyline, p'' is spatially closer to any query point q_i ($q_i \in Q$) than p. Since $q_j \in CH(Q)$, so $q_j \in Q$ as well. But according to the definition of independent regions, $D(p'', q_j) \geq D(p', q_j)$ since p'' is outside of $IR(p, q_j)$, which leads to a contradiction. Thus, this concludes the proof. □

The independent regions are determined by the independent region pivot and the convex hull of Q. The convex hull is uniquely determined by input query points Q; however, theoretically, the pivot can be arbitrarily selected. Since the independent regions specify the search region that contains spatial skyline candidates, an intuitive strategy of the data point selection is to select the data point that minimizes the total volume of its independent regions.

Figure 2 displays an example that utilizes independent regions in the spatial skyline evaluation in $\mathbb{R}^2$. The datasets P and Q consist of 8 data points and 4 query points, respectively. q_1, q_2, and q_3 are the convex points of the convex hull of Q. The three dashed circles indicate three independent regions generated by p_1 and the convex points. In this example, P is partitioned into three subsets, which are $P_1 = \{p_1, p_2, p_3, p_8\}$, $P_2 = \{p_1, p_4, p_5\}$, and $P_3 = \{p_1, p_5, p_6\}$. p_1 and p_8 are spatial skylines, because they are in the convex hull [23]. p_7 is outside all independent regions and can be discarded by mappers in the third phase. p_5 is in $IR(p_1, q_2)$ and $IR(p_1, q_3)$, thus p_5 is associated with both independent regions. Then, the spatial skylines in independent regions are calculated independently. Figure 4 shows an example of the pruning region in $IR(p_1, q_1)$ (the formal definition of pruning regions will be presented in Section 4.2.1). p_8 is a data point that is closer to q_1 than p_1. Thus, we create a pruning region $PR(p_8, q_1)$ (highlighted in gray) in $IR(p_1, q_1)$ to filter out data points dominated by p_8. In the example, p_3 falls in $PR(p_8, q_1)$, and can be discarded without being compared with p_2. Thus, p_2 is the only data point requiring spatial dominance test, comparing its distance to all convex points with the one of p_8. Our spatial skyline algorithm will be presented in Section 4.2.2.

4.2.1 Pruning Regions in Independent Regions

In the third MapReduce phase, a reduce function calculates spatial skylines of a set of data points in an independent region. In particular, the data points are comparing their distances to all convex points of $CH(Q)$ with all other data points (spatial skylines do not depend on non-convex points [23]), and the ones are discarded if they are spatially dominated in the same independent region. The data point comparison would be expensive when the number of convex points of $CH(Q)$ becomes large. Thus, to minimize the cost of the dominance test, we propose a pruning method that is able to efficiently filter out unqualified data points without accessing all convex points of $CH(Q)$. This method defines a pruning region in each independent region; if data points fall in the pruning region, they can be discarded because there must exist a data point dominating these data points. We will first illustrate the pruning regions in a 2-dimensional space, and then provide a formal definition and proof of the pruning regions in high-dimensional spaces.

Figures 6 and 7 show an example of a pruning region in $\mathbb{R}^2$. Given a query point q, two data points p and v, let L_{qx} be a line connecting q to any point $x \in \mathbb{R}^2$, and L_{vq} be the line of q and v. We build a 2-dimensional Cartesian coordinate system, in which q is the origin and L_{qx} is x axis. L_{qx} and L_{vq} partition $\mathbb{R}^2$ into two half-spaces, denoted by S^-_{qx} and S^+_{qx}, and S^-_{vq} and S^+_{vq}, respectively.

THEOREM 4.2. *If p and v satisfy*

$$\begin{aligned} &(1)\ v \in S^+_{qx} \text{ and } p \in S^-_{qx} \\ &(2)\ v.x \le p.x \\ &(3)\ D(v, q) > D(p, q) \end{aligned} \tag{4}$$

then p spatially dominates v with respect to any point q^*, $q^* \in S^-_{qx} \bigcap S^+_{vq}$.

PROOF. As a case of $p.x \ge 0$ shown in Figure 6, the three conditions indicate that (1) L_{qx} partitions v and p into two half-spaces, $v.y > 0$, $p.y < 0$; (2) if we create a line L_{pc} perpendicular to L_{qx}, then v is at the left side of L_{pc}; (3) v is outside of the circle centered at q with radius $D(p, q)$. The circle intersects with L_{pc} at p and b.

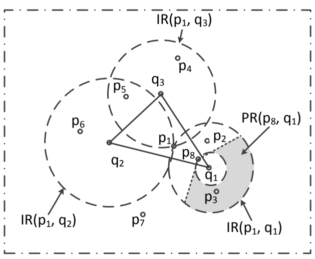

Figure 4: An example of Pruning Regions in $\mathbb{R}^2$.

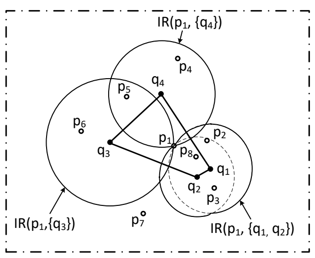

Figure 5: An example of merged Independent Regions in $\mathbb{R}^2$.

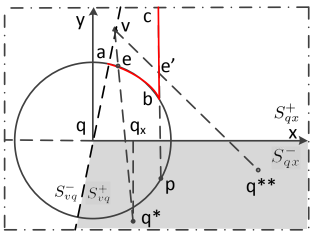

Figure 6: A pruning region using p and a visible facet L_{qx}.

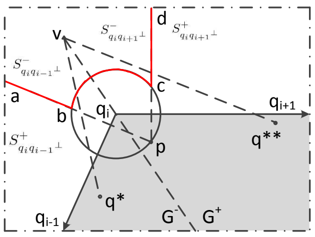

Figure 7: An example of $PR(p, q_i)$.

Given any data point q^* or q^{**} in $S^-_{qx} \bigcap S^+_{vq}$ (highlighted in gray), L_{vq^*} must intersect with either an arc from a to b (arc_{ab}) or a line from b to c (L_{bc}). If L_{vq^*} intersects with arc_{ab} at e, then we can get $D(p, q) = D(e, q)$ and $p.x > e.x$. Given a query point $q_x = \{q^*.x, 0\}$ on L_{qx}, then

$$\begin{aligned} D(e, q_x) &= \sqrt{(e.x - q^*.x)^2 + (e.y)^2} \\ &= \sqrt{D(e, q)^2 - 2 \cdot (e.x) \cdot (q^*.x) + (q^*.x)^2} \\ &> \sqrt{D(p, q)^2 - 2 \cdot (p.x) \cdot (q^*.x) + (q^*.x)^2} \\ &= \sqrt{(p.x - q^*.x)^2 + (p.y)^2} \\ &= D(p, q_x) \end{aligned} \tag{5}$$

thus, $D(p, q_x) < D(v, q_x)$. If q_x is moved to q^* ($q^*.y < 0$), then $D(p, q^*) < D(v, q^*)$ is also held. On the other hand, if $L_{vq^{**}}$ intersects with L_{bc} at e', then $D(p, q^{**}) < D(e', q^{**})$, because L_{qx} is the bisector line of p and b, and both p and q^{**} are in S^-_{qx}. Thus, $D(p, q^{**}) < D(e', q^{**}) \le D(v, q^{**})$. We can get the similar result in the case of $p.x < 0$. Therefore, p spatially dominates v with respect to any query point in $S^-_{qx} \bigcap S^+_{vq}$. □

In a 2-dimensional space, a convex hull is a convex polygon, in which each convex point has two adjacent convex points. Figure 7 shows three convex points q_{i-1}, q_i, and q_{i+1} of a convex hull $CH(Q)$. q_{i-1} and q_{i+1} are adjacent to q_i. Line segments $L_{q_iq_{i-1}}$ and $L_{q_iq_{i+1}}$ are two visible facets from a data point v outside $CH(Q)$ [9].

THEOREM 4.3. *In a 2-dimensional space, given a query point $q_i \in CH(Q)$ and a data point v outside $CH(Q)$, let $A^{\triangle}_{q_i}$ be a set of adjacent convex points of q_i, and p be an invisible data point from v. Each of the lines from p perpendicular to $L_{q_iq_j}$ ($q_j \in A^{\triangle}_{q_i}$) partitions the space into two closed half-spaces. Let $S^-_{q_iq_j{}^\perp}$ be the half space containing q_i. Then, any data point v outside $CH(Q)$ satisfying*

$$\begin{aligned} &(1)\ v \in S^-_{q_iq_j{}^\perp},\ q_j \in A^{\triangle}_{q_i} \\ &(2)\ D(v, q_i) > D(p, q_i) \end{aligned} \tag{6}$$

is spatially dominated by p with respect to Q.

PROOF. In Figure 7, L_{ab} and L_{cd} are two lines from p perpendicular to $L_{q_iq_{i-1}}$ and $L_{q_iq_{i+1}}$, respectively. L_{ab}, L_{cd}, and arc_{bc} separate v from the convex hull $CH(Q)$. L_{vq_i} partitions $CH(Q)$ into two closed half regions, G^- and G^+; all convex points are in either G^- or G^+. If a convex point q^* is in G^-, we can easily get $D(p, q^*) < D(v, q^*)$ by using Theorem 4.2. The similar result can be obtained in the case that any convex point q^{**} is in G^+. Thus, v is spatially dominated by p with respect to Q. □

After an illustration of pruning regions in $\mathbb{R}^2$, we extend the concept of pruning regions to high-dimensional spaces. In a d-dimensional space, a convex hull of query points Q can be represented by a set of half-spaces $\mathcal{H}$, where $CH(Q) = \bigcap_{h^+ \in \mathcal{H}} h^+$. The bisector hyper-plane of each half space contains a *(d-1)*- dimensional facet of the convex hull, which can be determined by a convex point and a subset of its adjacent convex points. The formal definition of the pruning regions is provided as follows.

Definition (*Pruning Regions*) In a d-dimensional space, given a convex hull of query points $CH(Q)$, a data point v outside $CH(Q)$, a visible convex point q, and an invisible data point p from v, let $A_q^{\triangle}$ be a set of adjacent convex points of q in facets, $h_{qq_j}^{\perp}$ be the *(d-1)*-dimensional hyper-plane that contains p and is perpendicular to L_{qq_j}, $q_j \in A_q^{\triangle}$. $h_{qq_j}^{\perp}$ partitions the space into two closed half-spaces; the one containing q is denoted by $S^-_{h_{qq_j}^{\perp}}$. Then any data point v outside $CH(Q)$ satisfying

$$\begin{aligned} &(1)\ v \in S^-_{h_{qq_j}^{\perp}},\ q_j \in A_q^{\triangle} \\ &(2)\ D(v,q) > D(p,q) \end{aligned} \tag{7}$$

is spatially dominated by p with respect to Q. The region containing all possible v is called a Pruning Region of p and q, denoted by $PR(p,q)$.

PROOF. The proof is by induction. The pruning region in a 2-dimensional space has been proven in Theorem 4.3. We assume that the pruning region is held in an *(i-1)*-dimensional space ($i \geq 3$), then, in an i-dimensional space, since v is outside $CH(Q)$, the line connecting v with any convex point q^* must intersect with a visible closed *(i-1)*-dimensional facet F of $CH(Q)$. The hyper-sphere centered at q with radius $D(p,q)$ and $h_{qq_j}^{\perp}$ ($q_j \in A_q^{\triangle}$) separate v from $CH(Q)$. If a ray from v to q^* intersects with the hyper-sphere at e earlier than any $h_{qq_j}^{\perp}(q_j \in A_q^{\triangle})$, then given any convex point $q_k \in A_q^{\triangle}$, we can build an i-dimensional Cartesian coordinate system, in which F is a hyper-plane ($x_i = 0$), $v.x_i > 0$, $p.x_i < 0$, and L_{qq_k} ($L_{qq_k} \in F$) is x axis. Any query point on L_{qq_k} can be represented by $\{x_1, 0, ..., 0\}$. Since $D(e,q) = D(p,q)$ and $e.x_1 < p.x_1$, given any query point q_x on L_{qq_k}, we can get

$$\begin{aligned} D(e,q_x) &= \sqrt{(e.x_1 - q_x.x_1)^2 + D(e, L_{qq_k})^2} \\ &= \sqrt{D(e,q)^2 - 2\cdot(e.x_1)\cdot(q_x.x_1) + (q_x.x_1)^2} \\ &> \sqrt{D(p,q)^2 - 2\cdot(p.x_1)\cdot(q_x.x_1) + (q_x.x_1)^2} \\ &= \sqrt{(p.x_1 - q_x.x_1)^2 + D(p, L_{qq_k})^2} \\ &= D(p,q_x) \end{aligned} \tag{8}$$

where $D(e, L_{qq_k})$ denotes the distance from e to the line L_{qq_k}. Thus, we can get that, given any query point q' satisfying D(p, q') $\leq$ D(e, q'), if q' is moved to q'' on any of the directions from q to its adjacent convex points in F, D(p, q'') < D(e, q'') is also held. So, p is closer to any query point in F than e. Since, $v.x_i > 0$, $p.x_i < 0$, and $q^*.x_i < 0$, so $D(p,q^*) < D(v,q^*)$. On the other hand, if a ray from v to q^* first intersects with $h_{qq_k}^{\perp}$ at e', let $q^{\circledast}$ be the center of the intersection of $h_{qq_k}^{\perp}$ and the hyper-sphere centered at q with radius D(p, q), $h_{qq_k}^{\perp}$ is an *(i-1)*-dimensional hyper-plane, in which $D(e', q^{\circledast}) > D(p, q^{\circledast})$, and $e' \in S^-_{h_{qq_t}}$, $q_t \neq q_k$, q_t, $q_k \in A_q^{\triangle}$, which satisfies the conditions in an *(i-1)*-dimensional space. Thus, $D(p, q^{\circledast}) < D(e', q^{\circledast})$; then $D(p,q^*) < D(e',q^*) \leq D(v,q^*)$. Therefore, this concludes the proof. $\square$

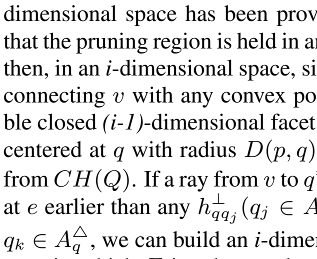

Figure 8: An example of visible facets of a convex hull in a 3-dimensional space.

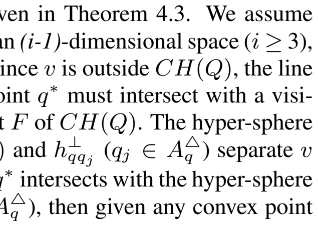

Figure 9: An example of a visible facet after a coordinate transformation.

Figure 8 shows an example of the convex hull of query points Q in a 3-dimensional space. v is a data point outside the convex hull. The line L_{vw_e} intersects with a visible facet F at e. F can be determined by three convex points q_{i-1}, q_i, and q_{i+1}. After a coordinate transformation, F is transformed to be on plane Z ($z = 0$), $v.z > 0$, and $p.z < 0$, as displayed in Figure 9. $L_{q_iq_{i+1}}$ is the x axis in plane Z. The area invisible from v, including p, is highlighted in gray. Two hyper-planes $h_{q_iq_{i-1}}^{\perp}$ and $h_{q_iq_{i+1}}^{\perp}$ perpendicular to $L_{q_iq_{i-1}}$ and $L_{q_iq_{i+1}}$ are highlighted in red. q_{i+1} and q_{i-1} are two elements of $A_{q_i}^{\triangle}$. If a ray from v to q^* first intersects with the sphere centered at q_i with radius $D(p,q_i)$ at e, then according to Equation 8, we can get that given any point q' on $L_{q_iq_{i+1}}$, $q'.x \geq q_i.x$, $D(p,q') \leq D(e,q')$, and moving the point on the direction from q_i to q_{i+1} with distance $\triangle d$ ($\triangle d > 0$) makes the point closer to p than e. The similar result can be obtained on the direction from q_i to q_{i-1}. Thus, any query point in the facet F is closer to p than e. Moreover, $e.z > 0$, $q.z < 0$, and $q^*.z < 0$, we can get that $D(p,q^*) < D(e,q^*) < D(v,q^*)$. On the other hand, if a ray from v to q^{**} first intersects with $h_{q_iq_{i+1}}^{\perp}$ at e', then $e'.x = p.x$, and $D(e',q_i) > D(p,q_i)$. Let q_i' be the intersection of $L_{q_iq_{i+1}}$ and $h_{q_iq_{i+1}}^{\perp}$, $D(e',q_i') > D(p,q_i')$. $h_{q_iq_{i-1}}^{\perp}$ intersects with $h_{q_iq_{i+1}}^{\perp}$ at a line, which contains p and partitions $h_{q_iq_{i+1}}^{\perp}$ into two closed half-spaces. q_i' and e' are in the same half space. By Theorem 4.3, $D(e',q_i') > D(p,q_i')$. Therefore, $D(v,q^{**}) \geq D(e,q^{**}) > D(p,q^{**})$, and v is spatially dominated by p with respect to Q.

4.2.2 Spatial Skyline Algorithm

With the concept of pruning regions, we present our spatial skyline algorithm used in reduce functions of the third phase. The input data points are grouped by their independent regions through the shuffle phase, and unqualified data points outside independent regions have been discarded in map functions. The fundamental idea of our method is to first eliminate data points by using pruning regions. If they are not in any pruning region, they are needed to compare with all other potential spatial skyline candidates for spatial dominance test.

The details of our method are described in Algorithm 1. The algorithm receives all data points in an independent region $IR(p,q_i)$, denoted by P_i, and the convex hull of query points Q. We use $chsky$ and $lssky$ to keep local spatial skylines inside and outside $CH(Q)$, respectively. PR abstracts pruning regions of the spatial skyline candidates. The union of $chsky$ and $lssky$ are output as spatial skylines in the independent region, which is a subset of the global spatial skylines of the query.

In particular, the algorithm first finds all the data points in $CH(Q)$. These data points are kept in $chsky$, and used to build pruning regions PR (from lines 4 to 11). $lssky$ temporarily maintains all data points outside $CH(Q)$. Then, each data point in $lssky$ is visited for the dominance test (from lines 12 to 20). If a data point falls in any pruning region, the data point will be removed from $lssky$. If the data point is outside the pruning regions, it needs to

Algorithm 1 Spatial Skyline Algorithm

```
Input: $P_i, CH(Q)$
Output: $lssky \cup chsky$
 1: $lssky = \emptyset$;
 2: $chsky = \emptyset$;
 3: $PR = \emptyset$;
 4: for $\forall p \in P_i$ do
 5:     if $p$ is inside $CH(Q)$ then
 6:         $chsky = chsky \cup \{p\}$;
 7:         $PR = PR \cup PR(p, q_i)$;
 8:     else
 9:         $lssky = lssky \cup \{p\}$;
10:     end if
11: end for
12: for $\forall p \in lssky$ do
13:     if $p$ is in $PR$ then
14:         $lssky = lssky - \{p\}$;
15:         Continue;
16:     end if
17:     if $\exists\, p' \in (chsky \cup lssky),\ p' \neq p,\ p' \prec^Q p$ then
18:         $lssky = lssky - \{p\}$;
19:     end if
20: end for
21: return $lssky \cup chsky$;
```

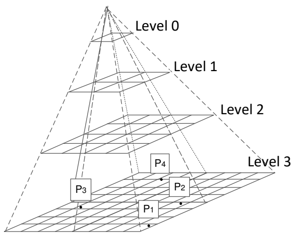

Figure 10: An example of $Grid(lssky \cup chsky)$**.**

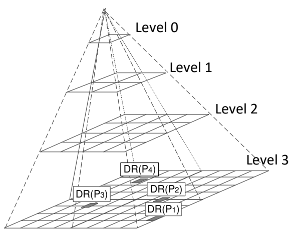

Figure 11: An example of $Grid(DR(lssky \cup chsky))$**.**

compare with all other data points in $chsky$ and $lssky$, and will be eliminated if it is dominated.

To minimize the cost of the dominance test in line 17, we use two multi-level grids, $Grid(lssky \cup chsky)$ and $Grid(DR(lssky \cup chsky))$, to maintain spatial skyline candidates and their dominator regions (defined in Section 3.1). The two grids are always synchronized; once there is a data point inserted into or removed from $Grid(lssky \cup chsky)$, $Grid(DR(lssky \cup chsky))$ is updated accordingly. Figures 10 and 11 display an example of the two grids. The cells at the bottom level keep the references of spatial skyline candidates and their dominator regions; parent cells maintain the proximity information of their child cells. In the dominance test of a new data point p, we first check if p is dominated by other data points. We calculate the dominator region of p, and visit $Grid(lssky \cup chsky)$ from top to bottom to see if there is a data point falling in the dominator region. The iteration can stop at any intermediate level when either of the two conditions is satisfied: (1) all cells intersecting with the dominator region do not contain any data point (p is not dominated by spatial skyline candidates in $lssky \cup chsky$); (2) a cell inside the dominator region contains a data point (p is dominated by the data point). If p is not dominated, then we visit $Grid(DR(lssky \cup chsky))$ in a similar manner to see if p dominates any data point in $lssky \cup chsky$. If p falls in the dominator region of p', then p' and its dominator region will be removed from both $Grid(lssky \cup chsky)$ and $Grid(DR(lssky \cup chsky))$.

4.3 Implementation Issues

In this subsection, we discuss three implementation issues in our solutions.

4.3.1 Independent Region Pivot Selection

In the second MapReduce phase, the search space is partitioned into a number of independent regions. The spatial skylines are calculated in parallel by reducers in the third MapReduce phase. The execution time of a parallel program is determined by the slowest process, and the spatial skyline algorithm takes longer on larger inputs. Thus, distributing the data points to reducers in a balanced manner is critical to our approach.

If the data points are uniformly distributed in the search space, the number of data points in an independent region is proportional to the volume of the independent region, which depends on the distance between the independent region pivot and the convex point. Theoretically, the point with equal distance to all convex points is the optimal independent region pivot, which could split data points in equal size. But the optimal pivot may not exist in irregular convex hull. Moreover, the point that minimizes the total volume of independent regions would be an alternative optimal pivot. However, the cost of finding the point is expensive. Thus, we turn to an approximation method in our implementation. After the convex hull is calculated, we choose the center of the Minimum Bounding Rectangle (MBR) of the convex hull as the independent region pivot. The experimental results of varying independent region pivots can be found in Section 5.6.

4.3.2 Independent Region Merging

In the third phase of our solution, a reducer processes data points in an independent region. The number of reducers needed in the spatial skyline calculation depends on the number of independent regions or the number of convex points in the convex hull of query points Q. Since the size of the convex hull would be large, the task maintenance and communication overhead in MapReduce framework would be unacceptably high.

Thus, there are two merging strategies that can be applied to our proposed solution if the number of independent regions is much greater than the number of available computing resources. In the strategies, we assume that objects are uniformly distributed in the search space. The smaller the total volume of independent regions is, the less the number of objects are processed in spatial skyline computation.

Shortest distance merging. In this method, we merge the closest pair of two neighboring independent regions. The distance of two independent regions is evaluated by the distance between the centers of the independent regions. We assume that there is higher possibility that two independent regions overlap with each other if they are close. Merging two overlapped independent regions may reduce the cost of spatial skyline computation for the following two reasons: (1) the objects in the overlapping region are fed to one reducer instead of two, which minimizes the total number of objects in the spatial dominance test; (2) the pruning regions of the independent regions are also merged; more objects could be eliminated without the dominance test. Take Figure 5 for example, q_1 and q_2 are the closest pair of convex points in the figure. $IR(p_1, q_1)$ and $IR(p_1, q_2)$ are merged, and the new independent region is denoted by $IR(p_1, \{q_1, q_2\})$. So, p_3 and p_8 are only processed by the reducer, which receives $IR(p_1, \{q_1, q_2\})$. The pruning region of $IR(p_1, \{q_1, q_2\})$ is PR(p_1, q_1) $\cup$ PR(p_1, q_2).

In our implementation, we iterate the convex hull in counter clockwise order, and calculate the distance between every pair of two consecutive independent regions. Let n be the number of computing resources available to the spatial skyline evaluation and m

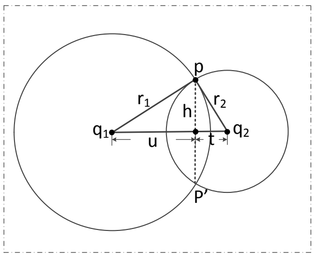

Figure 12: **Volume of overlapping region of two independent regions.**

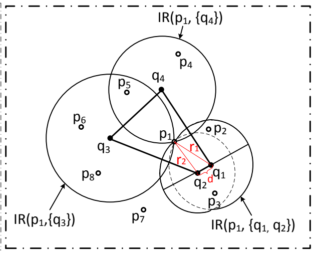

Figure 13: **An example of independent regions in a *2*-dimensional space.**

be the number of convex points, we will merge the top $m - n$ ($m \geq n$) closest pairs of the independent regions (the number of pairs of independent regions is equal to the number of convex points).

Threshold-based merging. An alternative strategy merges independent regions by considering the volume of the overlapping region of two independent regions. In this method, we visit the independent regions in counter clockwise order. Given two consecutive independent regions, we calculate the ratio of volume of the overlapping region of the two independent regions to the volume of the smaller independent region. If the ratio is higher than a specific threshold, the two independent regions will be merged. Another difference from the first method is that two or more independent regions may be merged if they are close to each other. The ratio can be defined as follows.

$$ratio(q_1, q_2) = \frac{Vol^d(IR(p_1, q_1)) \cap Vol^d(IR(p_1, q_2))}{Vol^d(IR(p_1, q_2))} \quad (9)$$

where $IR(p_1, q_1)$ and $IR(p_1, q_2)$ are two consecutive independent regions, $Vol^d(IR(p_1, q_2))$ denotes the volume of $IR(p_1, q_2)$ in a d-dimensional space, and $Vol^d(IR(p_1, q_1)) \geq Vol^d(IR(p_1, q_2))$.

Moreover, the volume of the overlapping region of two independent regions (two spheres) can be calculated as follows (See Figures 12 and 13).

$$Vol^d(IR(p_1, q_1) \cap IR(p_1, q_2)) = \int_{u_0}^{r_1} Vol^{d-1}(h)du + \int_{t_0}^{r_2} Vol^{d-1}(h)dt \quad (10)$$

where $Vol^{d-1}(h)$ denotes the volume of the sphere with radius h in a *(d-1)*-dimensional space, $h = (r_1^2 - u^2)^{1/2} = (r_2^2 - t^2)^{1/2}$. u_0 and t_0 are the lower bounds of the integrals, where $u_0 = \frac{r_1^2 - r_2^2 + D(q_1, q_2)^2}{2D(q_1, q_2)}$ and $t_0 = \frac{r_2^2 - r_1^2 + D(q_1, q_2)^2}{2D(q_1, q_2)}$. $D(q_1, q_2)$ denotes the distance between q_1 and q_2.

Figure 12 shows an example of the independent region merging in a 2-dimensional space. Line $l_{pp'}$ decomposes the overlapping region into two sub-regions. The length of $l_{pp'}$ is denoted by $V^1(h)$ = $2h$. If we move $l_{pp'}$ towards q_1 and q_2, respectively, then, the volume of the two sub-regions is the sum of integral of $V^{d-1}(h)$ in the overlapping area. In a d-dimensional space, $l_{pp'}$ becomes a sphere in a *(d-1)*-dimensional hyper-plane, and h is the radius of the sphere.

In a 2-dimensional space, $ratio(q_1, q_2)$ can be calculated as follows,

$$\begin{aligned} ratio(q_1, q_2) &= \frac{Vol^2(IR(p, q_1)) \cap Vol^2(IR(p, q_2))}{Vol^2(IR(p, q_1))} \\ &= \frac{\int_{u_0}^{r_1}(h)du + \int_{t_0}^{r_2}(h)dt}{Vol^2(IR(p, q_1))} \\ &= \frac{r^2 cos^{-1}(\frac{d^2+r_1^2-r_2^2}{2dr_2}) + r^1 cos^{-1}(\frac{d^2+r_2^2-r_1^2}{2dr_1})}{\pi {r_1}^2} \end{aligned} \quad (11)$$

4.3.3 Duplicate Elimination

The third issue is that our solution may produce duplicates since a data point may locate in two or more independent regions. If the data point is a spatial skyline, it will be written to the results of the query by multiple reducers. To eliminate the duplicates, we associate a unique independent region identifier to each data point, which indicates that the data point will be output as a spatial skyline by the reducer which processes data points in the independent region. Reducers processing data points in other independent regions will not output the data point even if it is a spatial skyline. Take Figure 4 as an example, p_5 is a data point in $IR(p_1, q_2)$ and $IR(p_1, q_3)$. If the identifier of $IR(p_1, q_2)$ is associated with p_5, and p_5 is a spatial skyline, p_5 is output only by the reducer processing data points in $IR(p_1, q_2)$.

5. EXPERIMENTAL VALIDATION

In this section, we evaluate the performance of the proposed MapReduce-based solution over synthetic and real-word datasets. Our proposed algorithm is denoted by $PSSKY$-G-IR-PR, which combines the concepts of independent regions, pruning regions, and multi-level grid data structure for efficient query evaluation. Since none of the existing solutions can be easily extended to address spatial skyline queries in parallel, we developed two single-phase MapReduce-based solutions as baselines, $PSSKY$ and $PSSKY$-G. $PSSKY$ applies a random data partitioning method to split data points. Each mapper uses BNL to produce local spatial skylines by comparing every pair of data points, and a reducer merges the local results and outputs the global spatial skylines. $PSSKY$-G works similarly to $PSSKY$ except that $PSSKY$-G utilizes multi-level grid data structure for efficient spatial dominance test. Since all three solutions use the same algorithm in convex hull computation, we will focus primarily on the investigation of the overall performance of solutions and the effect of independent regions and pruning regions on spatial skyline computation in the second and third MapReduce phases. All solutions were implemented in Java on Hadoop 2.6, which is an open source implementation of the MapReduce framework [1].

In the experiments, the real-word datasets were downloaded from Geonames [1]. We retrieved 11 million objects (streams, schools, etc.) in the United States, and used them as data points and query points. The data points in our synthetic datasets are randomly generated under uniform distribution in a 2-dimensional space. Similarly with [23], the query points were also generated in a specified region at the center of the search space. By default, there are 10 convex points in the convex hull of query points. The area covered by the Minimum Bounding Rectangle (MBR) of query points is fixed at 1% of the search space. The experiments were conducted on a 12-node shared-nothing cluster. Each node is equipped with 19 Intel Xeon 2.2 GHz processors and 128 GBytes of memory. All nodes are connected by GigaBit Ethernet network. All results were recorded after the system model reached a steady state.

[1]http://www.geonames.org/

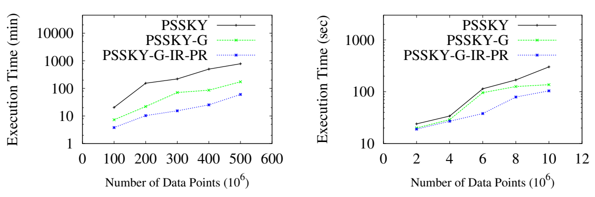

(a) Synthetic datasets. (b) Real-world datasets.

Figure 14: The overall execution time of the three solutions by varying dataset cardinality.

5.1 Scalability with Cardinality

First of all, we evaluate the effect of data cardinality on all three solutions. We vary the cardinality of both synthetic and real-world datasets from 100 to 500 million and 2 to 10 million data points, respectively. As Figure 14 displays, the execution time of all solutions increase when the datasets grow. The growth rate of $PSSKY$-G-IR-PR over synthetic datasets is lower than $PSSKY$ and $PSSKY$-G. In addition, on average, $PSSKY$-G-IR-PR executes around 90% faster than $PSSKY$ and 32% faster than $PSSKY$-G, respectively. The reason is that $PSSKY$-G-IR-PR is able to parallelize the spatial skyline evaluation by applying the concept of independent regions and efficiently filter out unqualified data points in pruning regions. Moreover, a performance improvement was observed when comparing $PSSKY$-G with $PSSKY$, because the multi-level grid data structure is employed to efficiently access the proximity information of data points for the dominance test.

5.2 Effect of Independent Regions and Pruning Regions on Spatial Skyline Algorithms

To evaluate the effectiveness of independent regions and pruning regions on the query evaluation, we compare the execution time of spatial skyline computation in $PSSKY$-G-IR-PR (the execution time of reducers in the third MapReduce phase) with the ones in $PSSKY$ and $PSSKY$-G. The cardinality of synthetic and real-world datasets varies from 100 to 500 million and 2 to 10 million data points.As Figure 15 shows, the execution time of all solutions increase when the datasets grow. The execution time of $PSSKY$ increases rapidly due to high complexity of spatial skyline computation. The growth rate of $PSSKY$-G-IR-PR is the lowest, because all data points can be processed in parallel and a significant portion of data points can be discarded without dominance test. Moreover, the reducer that merges spatial skylines becomes a bottleneck in $PSSKY$ and $PSSKY$-G, which consumes 50% to 90% of the total execution time over large synthetic and real-world datasets.

5.3 Effect of Number of Nodes

We evaluate the speedup of proposed solutions by scaling up the size of our cluster. The real and uniform datasets are fixed at 10 million and 100 million objects. The cardinality of cluster nodes varies from 2 to 12.

In Figure 17, the execution time of all solutions drops as the size of the cluster increases. As expected, $PSSKY$ always consumes more execution time than $PSSKY$-G and $PSSKY$-G-IR-PR while scaling up the cluster. On average, $PSSKY$-G-IR-PR enjoys the highest dropping rate. Take experiments on real world data for example, $PSSKY$-G-IR-PR drops 34.35% when scaling up to 8 nodes, PSSKY-G only drops 27%; the dropping rate of $PSSKY$ is constantly lower than 20% in all experiments. The reason is that more map or reduce tasks can be executed in parallel with more computing resources. However, even all three methods will take advantage of mapper parallelism, only reducers of $PSSKY$-G-IR-PR run in parallel, because the global region is partitioned into independent regions; the skyline results in each independent region do not depend on the ones in other independent regions.

For both synthetic and real data, $PSSKY$-G-IR-PR performs approximately 50% better than $PSSKY$-G and 80% better than $PSSKY$ in terms of execution time.

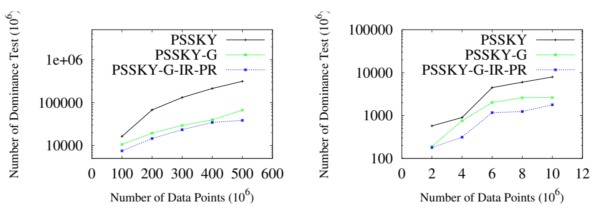

(a) Synthetic datasets. (b) Real-world datasets.

Figure 16: The number of dominance test by varying dataset cardinality.

5.4 Effect of Pruning Regions

We also evaluate the effect of pruning regions by comparing the number of dominance tests among three solutions. The cardinality of synthetic and real-world datasets varies from 100 to 500 million and 2 to 10 million data points. Figure 16 displays the number of dominance test in the three solutions over the datasets. As expected, $PSSKY$ always suffers from more dominance tests than $PSSKY$-G and $PSSKY$-G-IR-PR. Using multi-level grid data structure can reduce the cost of the dominance test, because, instead of access all data points, $PSSKY$-G only needs to visit data points in the cells that intersect with dominator regions of other data points. Moreover, the effect of pruning regions can be observed by comparing the results of $PSSKY$-G and $PSSKY$-G-IR-PR. Although data points locating at two or more independent regions may introduce subtle overhead in data point comparison, $PSSKY$-G-IR-PR can save more time in the dominance test by utilizing the concept of pruning regions. According to our experiments, there are a small number of duplicate data points generated

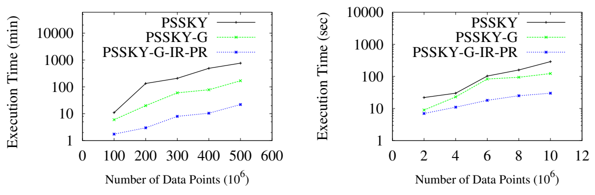

(a) Synthetic datasets. (b) Real-world datasets.

Figure 15: The execution time of spatial skyline algorithms by varying dataset cardinality.

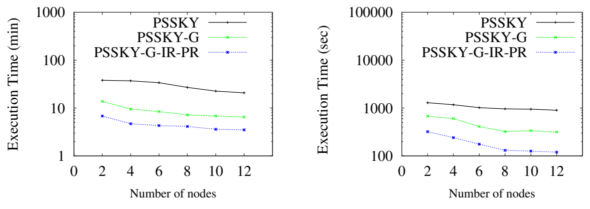

(a) Synthetic datasets. (b) Real-world datasets.

Figure 17: The overall execution time of the three solutions by varying nodes cardinality.

Table 2: Effectiveness of pruning regions by varying dataset cardinality.

Synthetic DataSets	Number of Data Points (million)				
	100	200	300	400	500
	27%	27%	27%	27%	27%

Real-world DataSets	Number of Data Points (million)				
	2	4	6	8	10
	10%	10%	9%	9%	8%

by $PSSKY$-G-IR-PR. Combining the experiments shown in Figure 15, $PSSKY$-G-IR-PR only takes a few minutes longer if there are additional 100 million dominance test are performed by $PSSKY$-G-IR-PR. Note that these dominance tests may be conducted in parallel in $PSSKY$-G-IR-PR.

Table 2 shows the power of pruning regions in terms of data point reduction rate by varying cardinality of datasets. The reduction rate is defined by the average percentage of data points eliminated by pruning regions in independent regions. We find that around 27% of data points in synthetic datasets fall in pruning regions, and can be discarded by $PSSKY$-G-IR-PR while there are around 9% of real-world data points that can be pruned without the dominance test. Moreover, the object elimination rate is slightly changed for large real-world datasets. The reason is that the number of data points varies in the experiments, but the number of query points and its convex hull are fixed. Theoretically, if data points are uniformed distributed, the effectiveness of the Pruning Region only depends on the volume of Pruning Regions. Increasing the density of data points over a large data point datasets does not help much to generate larger pruning regions. Thus, the reduction rate over synthetic datasets remains unchanged, and there is slight change in the reduction rate over real-world datasets due to the non-uniform distribution of data points.

Table 3 shows the power of pruning regions in terms of data point reduction rate by varying the distribution of data points. We replace 5%, 10%, 15%, and 20% of uniform data points with anti-correlated data points. For example, the experiments performed over datasets with 20% anti-correlated and 80% uniform data points are displayed in the first row of the results in Table 3. We find that the reduction rate remains the same over datasets under the same distribution of data points. Moreover, when 20% of anti-correlated data points are generated in datasets, only 2% difference is observed in the experiments, which tells us that the ratio of the volume of independent regions and pruning regions to that of the search space is small. In other words, if 20% data points are moved to the central area of the search space, there are only 2% of data points moved outside the pruning regions.

5.5 Effect of Query Points

We investigate the effect of the area covered by the convex hull of query points on the solutions in this subsection. We fix the size of data points at 100 million. The ratio of the area covered by the MBR of query points to the search space ranges from 1% to 2.5%. The number of Convex Hull query points selected for real-world datasets are 10, 14, 17, and 23, and that for synthetic datasets are 10, 12, 14, and 16, respectively. Figure 18 displays the overall execution time of solutions over synthetic and real-world datasets. The ratios of the MBR of the convex hull of query points are indicated by x axis. Intuitively, a larger convex hull may help to reduce the cost of the dominance test because more data points would locate in the convex hull, and can be output as spatial skylines without dominance test. However, our experimental results show that the entire process of query evaluation takes longer. The reason is that there are more data points in the search region, and the number of data points requiring dominance test becomes larger. Take Figure 2 for example, a convex hull is represented by q_1, q_2, and q_3. p_1 is used to generate three independent regions. If the convex hull grows larger, the area covered by the three independent regions will become larger accordingly. Thus, more data will be located in the independent regions, and be processed by reducers in the third MapReduce phase.

The evidence is also displayed in Figure 19 and 20. Figure 19 shows the execution time of spatial skyline computation and the number of dominance tests grow rapidly when the MBRs of the convex hull of query points cover larger areas. A similar results are observed in terms of the number of dominance test in Figure 20.

Table 3: Effectiveness of pruning regions by varying dataset distribution.

DataSets	Number of Data Points (million)				
	100	200	300	400	500
20% anti-correlated	24%	24%	24%	24%	24%
15% anti-correlated	24.7%	24.7%	24.7%	24.7%	24.7%
10% anti-correlated	25.3%	25.3%	25.3%	25.3%	25.3%
5% anti-correlated	26%	26%	26%	26%	26%

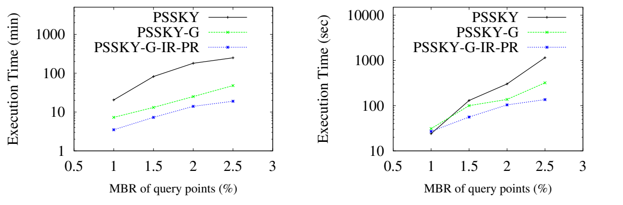

(a) Synthetic datasets. (b) Real-world datasets.

Figure 18: The overall execution time of the three solutions by varying the MBR of the convex hull of query points.

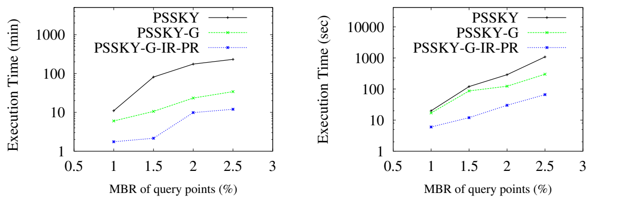

(a) Synthetic datasets. (b) Real-world datasets.

Figure 19: The execution time of spatial skyline algorithms by varying the MBR of the convex hull of query points.

5.6 Effect of Independent Region Pivot Selection

We investigate the effect of independent region pivot selection on the query evaluation by varying the pivot on real world datasets. We

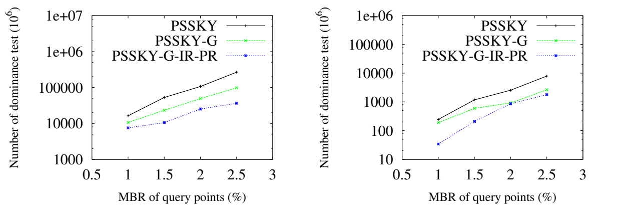

(a) Synthetic datasets. (b) Real-world datasets.

Figure 20: The number of dominance test in the three solutions by varying the MBR covered by query points.

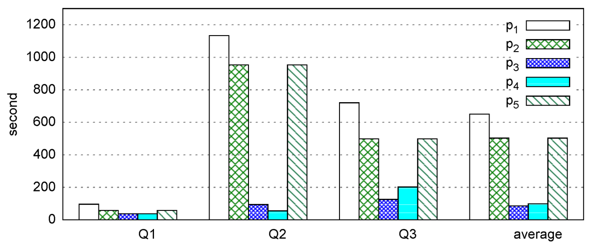

Figure 21: The execution time of $PSSKY\text{-}G\text{-}IR\text{-}PR$ by varying independent region pivots.

randomly choose three query dataset in such a way that the convex hull of the query points is in random shape. Figure 20 shows the execution time of the query when the pivot locates at the query points with minimum and maximum y-coordinate values (p_5 and p_1), and the center of $MBR(CH(Q))$ (p_3). Two additional pivots are selected at the midpoint of the line of p_1 and p_3, and the line of p_3 and p_5. The two pivots are denoted by p_2 and p_4, respectively. In general, p_3 is closer to the optimal pivot than other four pivots, and $PSSKY\text{-}G\text{-}IR\text{-}PR$ runs faster when p_3 is selected as the independent region pivot.

6. CONCLUSION AND FUTURE WORK

In this paper, we propose an advanced parallel spatial skyline solution utilizing MapReduce framework. Given a set of data points and a set of query points, our approach first calculates the convex hull of the query points. Then, we propose a novel concept of independent regions; the input data points are partitioned by their associated independent regions. Unqualified data points outside independent regions can be eliminated without the dominance test. Finally, all spatial skylines in independent regions are calculated in parallel, and the global spatial skylines are the union of local spatial skylines. Moreover, to avoid high cost of data point comparison, we propose a concept of pruning regions, in which objects can be discarded without comparing their distance to all convex hull query points. We demonstrate the efficiency and effectiveness of the proposed solution through extensive experiments on large-scale real-world, and synthetic datasets.

We plan to extend the proposed parallel solution to address spatial skyline queries on road networks. Theoretically, the concepts of independent regions and pruning regions can be applied in the space of road networks. However, more investigation is needed to evaluate the cost of calculating the independent regions and pruning regions. Due to variety of data distribution, it is also interesting to study the pruning power of pruning regions on road networks.

Acknowledgments

This research has been funded in part by the National Science Foundation grants IIS-1618669 (III) and ACI-1642133 (CICI).

References

[1] Apache Hadoop. `http://hadoop.apache.org`.

[2] F. N. Afrati, P. Koutris, D. Suciu, and J. D. Ullman. Parallel skyline queries. In *ICDT*, pages 274–284, 2012.

[3] W.-T. Balke, U. Güntzer, and J. X. Zheng. Efficient Distributed Skylining for Web Information Systems. In *EDBT*, pages 256–273, 2004.

[4] S. Börzsönyi, D. Kossmann, and K. Stocker. The Skyline Operator. In *ICDE*, pages 421–430, 2001.

[5] B. Chazelle. An optimal convex hull algorithm in any fixed dimension. *Discrete & Computational Geometry*, 10(1):377–409, 1993.

[6] L. Chen, K. Hwang, and J. Wu. Mapreduce skyline query processing with a new angular partitioning approach. In *IPDPS Workshops*, pages 2262–2270, 2012.

[7] J. Chomicki, P. Godfrey, J. Gryz, and D. Liang. Skyline with Presorting. In *ICDE*, pages 717–719, 2003.

[8] A. Cosgaya-Lozano, A. Rau-Chaplin, and N. Zeh. Parallel Computation of Skyline Queries. In *HPCS*, page 12, 2007.

[9] M. de Berg, O. Cheong, M. van Kreveld, and M. Overmars. *Computational Geometry: Algorithms and Applications*. Springer, 3rd edition, 2008.

[10] J. Dean and S. Ghemawat. MapReduce: simplified data processing on large clusters. *Commun. ACM*, 51(1):107–113, Jan. 2008.

[11] A. Eldawy, Y. Li, M. F. Mokbel, and R. Janardan. CG_Hadoop: Computational Geometry in MapReduce. In *SIGSPATIAL*, pages 294–303, 2013.

[12] X. Han, J. Li, D. Yang, and J. Wang. Efficient Skyline Computation on Big Data. *IEEE Trans. Knowl. Data Eng.*, 25(11):2521–2535, 2013.

[13] K. Hose and A. Vlachou. A survey of skyline processing in highly distributed environments. *VLDB J.*, 21(3):359–384, 2012.

[14] Z. Huang, C. S. Jensen, H. Lu, and B. C. Ooi. Skyline Queries Against Mobile Lightweight Devices in MANETs. In *ICDE*, page 66, 2006.

[15] H. Köhler, J. Yang, and X. Zhou. Efficient parallel skyline processing using hyperplane projections. In *SIGMOD Conference*, pages 85–96, 2011.

[16] D. Kossmann, F. Ramsak, and S. Rost. Shooting Stars in the Sky: An Online Algorithm for Skyline Queries. In *VLDB*, pages 275–286, 2002.

[17] K. Mullesgaard, J. L. Pedersen, H. Lu, and Y. Zhou. Efficient Skyline Computation in MapReduce. In *EDBT*, 2014.

[18] A. Okcan and M. Riedewald. Processing theta-joins using MapReduce. In *SIGMOD Conference*, pages 949–960, 2011.

[19] D. Papadias, Y. Tao, G. Fu, and B. Seeger. Progressive skyline computation in database systems. *ACM Trans. Database Syst.*, 30(1):41–82, 2005.

[20] Y. Park, J.-K. Min, and K. Shim. Parallel computation of skyline and reverse skyline queries using mapreduce. *PVLDB*, 6(14):2002–2013, 2013.

[21] J. B. Rocha-Junior, A. Vlachou, C. Doulkeridis, and K. Nørvåg. AGiDS: A Grid-Based Strategy for Distributed Skyline Query Processing. In *Globe*, pages 12–23, 2009.

[22] A. D. Sarma, A. Lall, D. Nanongkai, and J. J. Xu. Randomized multi-pass streaming skyline algorithms. *PVLDB*, 2(1):85–96, 2009.

[23] M. Sharifzadeh and C. Shahabi. The Spatial Skyline Queries. In *VLDB*, pages 751–762, 2006.

[24] W. Son, M. Lee, H. Ahn, and S. Hwang. Spatial Skyline Queries: An Efficient Geometric Algorithm. In *SSTD*, pages 247–264, 2009.

[25] K.-L. Tan, P.-K. Eng, and B. C. Ooi. Efficient Progressive Skyline Computation. In *VLDB*, pages 301–310, 2001.

[26] R. Vernica, M. J. Carey, and C. Li. Efficient parallel set-similarity joins using MapReduce. In *SIGMOD Conference*, pages 495–506, 2010.

[27] A. Vlachou, C. Doulkeridis, and Y. Kotidis. Angle-based space partitioning for efficient parallel skyline computation. In *SIGMOD Conference*, pages 227–238, 2008.

[28] P. Wu, C. Zhang, Y. Feng, B. Y. Zhao, D. Agrawal, and A. El Abbadi. Parallelizing Skyline Queries for Scalable Distribution. In *EDBT*, pages 112–130, 2006.

[29] B. Zhang, S. Zhou, and J. Guan. Adapting skyline computation to the mapreduce framework: Algorithms and experiments. In *DASFAA Workshops*, pages 403–414, 2011.

[30] C. Zhang, F. Li, and J. Jestes. Efficient parallel kNN joins for large data in MapReduce. In *EDBT*, pages 38–49, 2012.

[31] J. Zhang, X. Jiang, W.-S. Ku, and X. Qin. Efficient Parallel Skyline Evaluation using MapReduce. *IEEE Trans. Parallel Distrib. Syst.*, 2015.

[32] S. Zhang, N. Mamoulis, and D. W. Cheung. Scalable skyline computation using object-based space partitioning. In *SIGMOD Conference*, pages 483–494, 2009.